International Journal of Medical Microbiology 309 (2019) 151327

Contents lists available at ScienceDirect

International Journal of Medical Microbiology

journal homepage: www.elsevier.com/locate/ijmm

Role of the *Streptomyces* spore wall synthesizing complex SSSC in differentiation of *Streptomyces coelicolor* A3(2)

B. Vollmer[a], N. Steblau[a], N. Ladwig[a], C. Mayer[a], B. Macek[b], L. Mitousis[a], S. Sigle[a], A. Walter[a], W. Wohlleben[a], G. Muth[a,*]

[a] *Interfakultaeres Institut für Mikrobiologie und Infektionsmedizin Tuebingen IMIT, Mikrobiologie/Biotechnologie, Eberhard Karls Universitaet Tuebingen, Auf der Morgenstelle 28, 72076, Tuebingen, Germany*

[b] *Proteome Center Tuebingen, Interfakultaeres Institut für Zellbiologie, Eberhard Karls Universitaet Tuebingen, Auf der Morgenstelle 15, 72076 Tübingen, Germany*

ARTICLE INFO

Keywords:
Sporulation
Cell envelope
eSTPK
Phosphorylation
Cell wall glycopolymers

ABSTRACT

A crucial stage of the *Streptomyces* life cycle is the sporulation septation, a process were dozens of cross walls are synchronously formed in the aerial hyphae in a highly coordinated manner. This process includes the remodeling of the spore envelopes to make *Streptomyces* spores resistant to detrimental environmental conditions. Sporulation septation and the synthesis of the thickened spore envelope in *S. coelicolor* A3(2) involves the *Streptomyces* spore wall synthesizing complex SSSC. The SSSC is a multi-protein complex including proteins directing peptidoglycan synthesis (MreBCD, PBP2, Sfr, RodZ) and cell wall glycopolymer synthesis (PdtA). It also includes two eukaryotic like serin/threonine protein kinases (eSTPK), PkaI and PkaH, which were shown to phosphorylate MreC. Since unbalancing phosphorylation activity by either deleting eSTPK genes or by expressing a second copy of an eSTPK gene affected proper sporulation, a model was developed, in which the activity of the SSSC is controlled by protein phosphorylation.

1. Introduction

Streptomycetes are Gram-positive soil dwelling bacteria that are distinguished from most other bacteria by their mode of growth and their complex life cycle. A germinating spore develops one or two germ tubes which elongate by apical tip extension. Under optimal conditions the tips grow at a rate of 20 µm h^{-1} (Jyothikumar et al., 2008). Peptidoglycan (PG) incorporation at the tips is directed by the polarisome composed of the cytoskeletal proteins DivIVA, Scy and FilP (Fuchino et al., 2013). In a distance of 10–40 µm to the tip new branching points are established by small DivIVA clusters that splitted off from the tip assemblies. As the multiply branched mycelium develops, vegetative septal cross walls are built at irregular distances, often close to branching points (Flardh, 2003, Flardh et al., 2012; Richards et al., 2012).

Upon partial nutrient limitation, *Streptomyces* enters the next stage of its life cycle. Controlled by multiple *bld* genes (for bald, unable to form aerial hyphae), so-called aerial hyphae are formed on the surface (Flardh and Buttner, 2009; Salerno et al., 2013). The aerial hyphae are unbranched and usually evade from the vegetative mycelium by growing into the air, although some species, like *S. venezuelae* and *S. griseus* are able to differentiate in liquid culture (Schlimpert et al., 2016). The membranes of aerial hyphae are equipped with bacterial sterols, the hopanoids, unlike those of vegetative hyphae, probably to resist oxygen stress (Poralla et al., 2000). To lower the surface tension, the aerial mycelium is covered by an amyloidal layer of hydrophobic proteins consisting of rodlin and chaplins, which self-aggregate to characteristic rodlet structures (Claessen et al., 2004; Elliot et al., 2003). A hierarchic cascade of *whi* genes, encoding several transcriptional regulators control initiation of multiple cell division events and conversion of aerial hyphae into spore chains (Kelemen and Buttner, 1998; Bush et al., 2015). Replication of the chromosome is upregulated, generating multi-genomic aerial hyphae (Ruban-Ośmiałowska et al., 2006). Then, positioned by SsgB, the bacterial tubulin homolog FtsZ assembles to cytokinetic Z-rings at regular intervals (Willemse et al., 2011). FtsZ rings are stabilized by two dynamin-like proteins, DynA and DynB, and the stabilization of the newly formed Z-rings is crucial for completion of septum synthesis (Schlimpert et al., 2017). Proper

Abbreviations: PG, Peptidoglycan; CWG, Cell Wall Glycopolymer; PDP, Polydiglycosylphosphate; Kdn, 2-keto-3-deoxy-D-glycero-D-galacto-nononic acid; Gal, Galactose; MurNAc, N-acetylmuramic acid; GlcNAc, N-acetylglucosamine; BACTH, Bacterial Adenylate Cyclase based Two-Hybrid system; eSTPK, eukaryotic like serin/threonine protein kinase

* Corresponding author.
E-mail address: gmuth@biotech.uni-tuebingen.de (G. Muth).

https://doi.org/10.1016/j.ijmm.2019.07.001
Received 28 December 2018; Received in revised form 2 July 2019; Accepted 7 July 2019

synthesis of the sporulation septa and the spore envelope involves in addition further cytoskeletal proteins, the actin homologues MreB and Mbl (Heichlinger et al., 2011). With the help of ParAB, FtsK, the FtsK-like SffA and SmeA, which localizes SffA to the sporulation septa, the multiple chromosome copies segregate into the spore compartments (Wang et al., 2007; Ausmees et al., 2007; Jakimowicz et al., 2005). After thickening of the spore envelope uninucleoid spores are released, giving rise to a new life cycle.

2. Identification of genes involved in sporulation of *S. coelicolor* A3(2)

Like other streptomycetes, *S. coelicolor* A3(2) contains an *mre* gene cluster, encoding the key components of the lateral wall synthesizing complex for elongation growth of rod-shaped bacteria (Divakaruni et al., 2007): MreB, MreC, MreD, PBP2, and the FtsW-like SEDS (*shape, elongation, division, and sporulation*) family protein Sfr (Kleinschnitz et al., 2011a; Mazza et al., 2006). FtsW was recently shown to act as a PG-polymerase, thereby forming a complex with its partner PBP to polymerize lipid II into PG (Meeske et al., 2016; Taguchi et al., 2019). The actin-like MreB forms discrete small structures along the bacerial cell membrane that move independently arround the cell circumference (Dominguez-Escobar et al., 2011; Garner et al., 2011). These MreB patches coordinate location of extracytoplasmic cell wall synthesis via interaction with the transmembrane linker RodZ (Morgenstein et al., 2015). Although the depletion phenotype of *mreC* and *mreD* is similar to that of *mreB*, the molecular function of MreC and MreD in elongation growth is still mysterious (Kruse et al., 2005).

The “rod-shape-determining” *mre* genes of *S. coelicolor* A3(2) have a specific role in proper sporulation, but are dispensable for vegetative growth (Kleinschnitz et al., 2011a; Mazza et al., 2006, Burger et al., 2000). Spores of single mutants were sensitive to detrimental environmental conditions, like heat, desiccation, high osmolarity, or cell wall damage by lysozyme or vancomycin, indicating that the integrity of the spore envelope was impaired. Moreover, fusion proteins of MreB and the MreB-like protein Mbl of *S. coelicolor* A3(2) were localized to sites of spore wall synthesis during the conversion of aerial hyphae into spore chains (Heichlinger et al., 2011). These data suggested that the Mre proteins, which direct PG incorporation at the lateral wall during elongation growth of rod-shaped bacteria have a different role in *Streptomyces* than in other bacteria and are involved in the synthesis of the thickened spore envelope. Since the *Streptomyces* MreBCD, PBP2, and Sfr proteins show a similar protein-protein interaction pattern as their homologues from rod-shaped bacteria, the term “*Streptomyces* spore wall synthesizing complex (SSSC) was coined in analogy to the “lateral wall synthesizing complex” of rod-shaped bacteria (Kleinschnitz et al., 2011a).

To identify additional genes involved in the morphological differentiation of *S. coelicolor* A3(2), two distinct strategies were applied: i. Identification of interaction partners of SSSC proteins by bacterial two-hybrid analyses and ii. transposon mutagenesis.

3. Identification of additional SSSC proteins by bacterial two-hybrid analyses

Genomic libraries of *S. coelicolor* A3(2), generated either by enzymatic digest (Kleinschnitz et al., 2011a) or nebulization (Mehari and Muth, unpublished) of M145 DNA were screened with the **B**acterial **A**denylate **C**yclase based **T**wo-**H**ybrid system (BACTH, Karimova et al., 1998) for interaction partners of MreB, MreC, MreD, PBP2, Sfr, and RodZ (Kleinschnitz et al., 2011a, Mitousis and Muth, unpublished). Only for MreB, known to be poorly interacting in BACTH analyses (Formstone et al., 2008), no interaction partner was found. However, screening of the library with the other SSSC proteins delivered multiple interaction partners. Some of the interacting protein fragments were even fished with different bait proteins (Table 1). Many of these Mre-interaction partners have a role in proper sporulation, as it was demonstrated by gene inactivation studies. Deletion of *SCO1403, SCO2097, SCO2584*, *SCO6494,* or *SCO2578* (*pdtA*), originally annotated as hypothetical protein encoding genes and *SCO4778*, encoding the eukaryotic type serine/threonine kinase (eSTPK) PkaI, interfered with proper sporulation. In all mutants, spore chains were formed that contained irregular sized spores and spores with impaired integrity of the spore envelope (Muth, unpublished, Sigle et al., 2016a; Kleinschnitz et al., 2011a, b; Ladwig et al., 2015). Thus, the mutant phenotype validated the strategy to identify novel differentiation proteins via protein-protein-interactions with already known differentiation proteins and expanded the composition of the SSSC and its activities (see below).

Since the C-terminal end ($PkaI_{257-357}$) of the eSTPK PkaI was one of the most frequently fished prey polypeptides and was caught with MreC (8x), MreD (5x), PBP2 (1x), Sfr (6x), and RodZ (2x), a prominent role of PkaI in sporulation was suggested. A BACTH search for binding partners of the $PkaI_{257-357}$ interaction domain again revealed multiple proteins (Fig. 1, Table 1). The $PkaI_{257-357}$ interaction partners included BldB, AfsQ1, CrgA, or FtsH, which have a well-documented role in differentiation (Del Sol et al., 2003; Eccleston et al., 2002; Shu et al., 2009). Also, proteins were identified that were previously fished with one of the Mre proteins (e.g. SCO2097, SCO1403, SCO3110, SCO6494, SCO3754) (Ladwig et al., 2015). Moreover, the eSTPKs PkaD (SCO4777), encoded immediately next to *pkaI*, PkaI, and PkaA (SCO2974) were detected among the $PkaI_{257-357}$ interacting proteins.

In total, the BACTH screen identified several classes of interaction partners, revealing novel aspects of *Streptomyces* differentiation:

3.1. ABC-transporters

Strikingly, the SSSC seems to contain multiple (sugar) transporter proteins, in particular binding-protein-dependent transporters containing a Pfam BPD_transp_1 domain (SCO1057 (UgbA), SCO1064, SCO4141 (PstA), SCO5119, SCO5322 (DasB), and SCO5774 (GluD)). The ability to metabolize different sugars was already shown to influence differentiation and involvement of ABC transporters in proper sporulation of *Streptomyces* is well-documented (Colson et al., 2008; Nothaft et al., 2010; Seo et al., 2002; Ma and Kendall, 1994). Most interestingly were SCO3110 and SCO3754, which both were detected by their interaction with MreC and PkaI. SCO3110 contains doubled MacB_PCD (MacB-like periplasmic core domain) and FtsX domains, while SCO3754 contains a single MacB_PCD and two FtsX domains (Fig. 2). MacB is an antibiotic exporter that is distinguished from other ABC transporters in its transmission mechanism (Crow et al., 2017). MacB does not possess a central pore through which substrates might be passed, but operates through extracytoplasmic conformational change driven by cytoplasmic ATP hydrolysis. FtsEX was shown to be crucial for divisome assembly by forming a substrate-less ABC transporter involved in transmembrane signaling between cytoplasmic and periplasmic components of the cell division machinery in Gram-negative bacteria (Du et al., 2016).

3.2. Novel morphogenic proteins

SCO2097 was isolated from the genomic library with RodZ, MreC, MreD, and with Sfr (Kleinschnitz et al., 2011a). Additionally, SCO2097 interacted with the penicillin binding proteins PBP2, SCO3580, SCO3901 and FtsI. *SCO2097* encodes a signature protein, only occurring in actinomycetes and is located in the *ftsI* and *ftsZ* containing *division and cell wall cluster* (*dcw*). Although the exact function of the 135 aa membrane protein SCO2097 still has to be elucidated, the mutant phenotype indicating an impaired spore wall supported a role of SCO2097 in proper sporulation (Kleinschnitz et al., 2011a). SCO1403, interacting with RodZ, MreC and PkaI and SCO6494, interacting with MreD and PkaI encode membrane proteins of unknown function. Both genes were deleted from the chromosome of M145. The respective

Table 1
Interaction partners of SSSC proteins identified by BACTH screening of *S. coelicolor* A3(2) genomic libraries[*].

tag (protein)[§]	region (aa)	putative function	bait protein (isolation frequency)
ABC- transporter			
SCO1057 (UgpA)	24-108	ABC sugar permease,	MreC
SCO1058 (UgpE)	1-70	ABC transporter subunit	$PkaI_{257-357}$
SCO1064	113-149	sugar transporter subunit	PBP2
SCO3110	431-473	ABC-transporter subunit	MreC, $PkaI_{257-357}$
SCO3110	1-96	ABC transport system	MreC (2)
SCO3754	1-197	ABC transporter subunit	MreC, MreD (5),
SCO3754	1-184	ABC transporter subunit	$PkaI_{257-357}$
SCO4141 (PstA)	255-336	phosphate ABC transport permease	$PkaI_{257-357}$
SCO5119	8-94	ABC oligopeptide transporter	MreC
SCO5233 (DasB)	73-99	ABC Transporter	MreC
SCO5774 (GluD)	1-102	glutamate permease	MreC
Protein phosphorylation			
SCO2974 (PkaA)	474-523	eSTPK	MreC, $PkaI_{257-357}$ (2)
SCO3860	98-116	eSTPK	MreC
SCO4777 (PkaD)	400-548	serine/threonine protein kinase	$PkaI_{257-357}$ (2)
SCO4778 (PkaI)	257-357	eSTPK	Sfr (6), RodZ (2), PBP2, MreD (5), MreC (8), $PkaI_{257-357}$
SCO7326 (RsbU)	772-824	serine/threonine phosphatase	$PkaI_{257-357}$
Cell wall synthesis / differentiation			
SCO2097	21-120	membrane protein	MreD (6), RodZ (3), Sfr (29), $PkaI_{257-357}$ (35)
SCO1403	33-143	integral membrane protein	RodZ, MreC, $PkaI_{257-357}$ (5)
SCO2578 (PdtA)	176-246	LCP-CWG transferase	MreC (3), MreD (2)
SCO2584	145-228	membrane protein	MreC (3), Sfr
SCO2897	20-116	probable secreted PBP	$PkaI_{257-357}$
SCO3854 (CrgA)	1-84	septation inhibitor protein	$PkaI_{257-357}$
SCO4129 (CmdD)	51-108	sporulation	MreC
SCO4641	141-398	efflux protein, close to *murB*	$PkaI_{257-357}$
SCO4907 (AfsQ1)	122-225	pleiotropic transcriptional regulator	$PkaI_{257-357}$
SCO5039	608-716	bifunctional penicillin binding protein	MreC
SCO5587 (FtsH)	12-91	cell division protein	$PkaI_{257-357}$
SCO5723 (BldB)	1-98	pleiotropic regulator of differentiation	$PkaI_{257-357}$
SCO6374	215-257	bactoprenyl sugar transferase	MreC
SCO6374	298-478	bactoprenyl sugar transferase	$PkaI_{257-357}$
SCO6494	27-205	membrane protein	MreD, $PkaI_{257-357}$ (2)
Others			
SCO3218	20-71	*mbtH*-like, Cda cluster	$PkaI_{257-357}$
SCO3598	1-254	CPBP family metalloprotease	MreC
SCO4155	36-156	two component sensor protein	PBP2 (2), RodZ
SCO4597	1-249	two component sensor protein	MreC, MreD
SCO7048	13-306	delta fatty acid desaturase	MreD (5), PBP2
Hypothetical proteins			
SCO1385	1-246	hypothetical protein	Sfr
SCO1465	1-252	putative secreted protein	$PkaI_{257-357}$
SCO1610	129-176	hypothetical membrane protein	MreC
SCO1994	32-110	integral membrane protein	PBP2
SCO1829	27-96	putative membrane protein	$PkaI_{257-357}$ (2)
SCO2124	139-202	membrane protein	MreC (2), Sfr
SCO2169	61-212	putative integral membrane protein	$PkaI_{257-357}$ (2)
SCO2187	29-213	conserved hypothetical protein	MreD
SCO2255	13-178	putative membrane protein	$PkaI_{257-357}$
SCO2520	1-219	hypothetical protein	PBP2
SCO3146	9-58	putative secreted protein	$PkaI_{257-357}$
SCO3513	1-169	secreted protein	RodZ (2), Sfr, PBP2 (3)
SCO3927	19-199	membrane protein	MreD
SCO3940	1-238	putative transmembrane protein	$PkaI_{257-357}$
SCO4369	1-168	hypothetical protein	MreC
SCO4431	1-169	putative integral membrane protein	$PkaI_{257-357}$ (3)
SCO4732	13-286	membrane protein	MreC
SCO4811	390-438	hypothetical membrane protein	MreC
SCO4825	33-178	integral membrane protein	MreC, PBP2 (2)
SCO4846	236-307	putative integral membrane protein	$PkaI_{257-357}$
SCO5013	1-129	putative secreted protein	$PkaI_{257-357}$ (3)
SCO5142	1-119	secreted protein	MreC, RodZ, Sfr
SCO5148	114-306	putative membrane protein	$PkaI_{257-357}$
SCO5485	1-91	small hydrophobic membrane protein	$PkaI_{257-357}$
SCO5935	41-278	putative membrane protein	$PkaI_{257-357}$
SCO5993	49-144	putative membrane protein	$PkaI_{257-357}$
SCO6002	44-142	hypothetical membrane protein	MreC
SCO6074	4-203	putative integral membrane protein	$PkaI_{257-357}$
SCO6614	1-206	putative membrane protein	$PkaI_{257-357}$
SCO6771	1-39	small hydrophobic secreted protein	RodZ, Sfr
SCO6899	1-251	membrane protein	RodZ, Sfr, PBP2, $PkaI_{257-357}$
SCO7090	324-472	hypothetical membrane protein	MreC (2)
SCO7199	36-131	hypothetical membrane protein	MreC

(*continued on next page*)

Table 1 (*continued*)

tag (protein)[§]	region (aa)	putative function	bait protein (isolation frequency)
SCO7454	1-261	membrane protein	MreC
SCO7482	1-133	putative integral membrane protein	$PkaI_{257-357}$

* black letters indicate library generated by a partial Sau3A digest, grey letters mark a library containing nebulized DNA fragments.
§ bold letters indicate that the role in morphological differentiation is supported by experimental data.

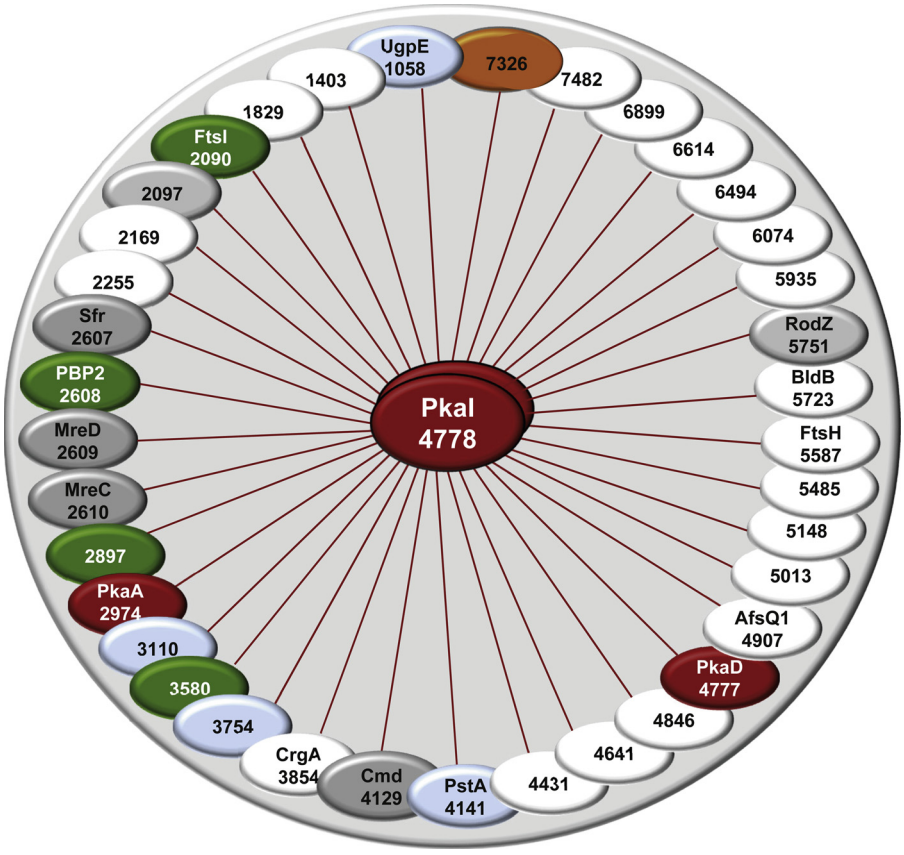

Fig. 1. Interaction pattern of PkaI. Interaction partners of the $PkaI_{257-357}$ interaction domain were identified by the screening of a genomic library with the bacterial two-hybrid system. SSSC proteins are shown in grey, ABC transporters in light blue, penicillin binding proteins in green, Ser/Thr protein kinases in red, and the putative Ser/Thr phosphatase SCO7326 in orange. The numbers refer to the SCO-numbers of the proteins. Self-interactions are indicated by double ellipses.

mutants were impaired in proper differentiation and formed aberrant spore chains containing non-viable spores, a phenotype characteristic for SSSC mutants (Muth et al., unpublished results).

3.3. Proteins involved in cell wall glycopolymer synthesis

Two of the proteins, SCO2578 and SCO2584 were predicted to be involved in the synthesis of cell wall glycopolymers (CWG), due to the location of the respective genes next to putative CWG genes. While SCO2584 represents an uncharacterized membrane protein, SCO2578 contains a LytR_cpsA_psr domain and is a predicted TagV homologous transferase, which anchors CWGs to the PG layer (see below). Inactivation of both genes resulted in the formation of aberrant spores with impaired spore envelopes (Kleinschnitz et al., 2011b; Sigle et al., 2016a).

4. Identification of novel differentiation genes by random transposon mutagenesis of *S. coelicolor* A3(2)

Most of the previously isolated differentiation mutants had quite severe defects causing white (*whi*) and bald (*bld*) phenotypes (Kelemen and Buttner, 1998; Bush et al., 2015). The mutants affected in SSSC

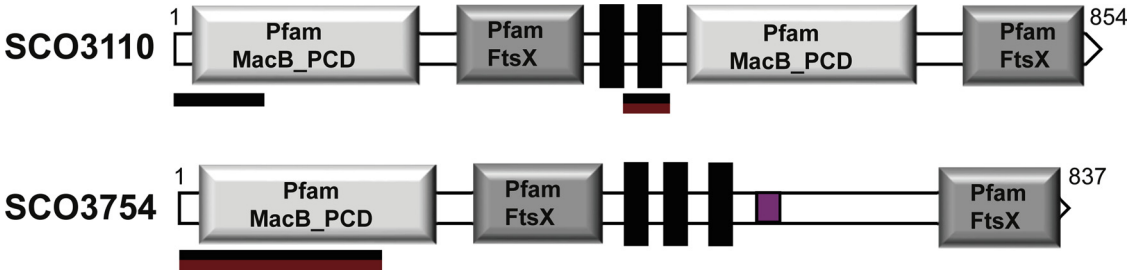

Fig. 2. Domain architecture of two uncommon ABC transporter components identified by their protein-protein interaction with MreC and PkaI. Domain architecture was determined with SMART (http://smart.embl-heidelberg.de/). The interacting regions with MreC (black) and PkaI (red) are indicated by horizontal bars. Regions of low compositional complexity are indicated in pink.

genes had been overseen in these previous screens, since their minor defect, aberrant spores with an impaired spore envelope, has no dramatic consequences for the colony morphology (Kleinschnitz et al., 2011, Ladwig et al., 2015).

To identify additional genes involved in morphological differentiation of *S. coelicolor* A3(2), transposon mutagenesis was performed (Muth et al., unpublished results). The transposon delivery vector pHL734 (Xu et al., 2017) was introduced into M145 protoplasts, yielding about 25.000 apramycin resistant transformants, where the mini-transposon consisting of the *E. coli* ori_{pMB1}, the apramycin resistance gene *aac(3)IV,* and the recognition sites of the hyperactive Tn*5* transposase has been inserted in the M145 genome. Transformants with altered colony morphology were directly picked from the transformation plates. Moreover, spores from the transformation plates were harvested and plated to single colonies on MS agar supplemented with 10.3% sucrose. Supplementation with 10.3% sucrose causes osmotic stress, which increases possible morphological defects. Colonies with aberrant morphology (e.g. retarded sporulation) were picked after 4 days of growth. To determine the transposon insertion sites, total DNA was isolated from ˜ 120 colonies and digested with the restriction endonuclease SalI, which does not cut within the mini transposon. After religation and transformation of *E. coli*, the plasmids isolated from apramycin resistant transformants were sequenced with primers corresponding to the ends of the transposon (Thoma and Muth, unpublished). Surprisingly, about 10% of the transposon mutants were cointegrates, where the whole pHL734 plasmid had been inserted. This was unexpected, since Tn5 is known to "jump" via a cut-and-paste mechanism, not involving the formation of cointegrates (Reznikoff, 2008). Since in these mutants, the present transposase could cause secondary mutations by subsequent transposition events, these mutants were excluded from further analyses. The other mutants (Table 2) revealed interesting aspects of *Streptomyces* sporulation.

Several mutants were obtained which had a transposon insertion in genes already reported to be involved in sporulation, e.g. the regulatory *wblA, devA, adpA,* or *abrA1* genes. Quite unexpectedly and not detected in previous screenings for differentiation mutants, many mutants had insertions in nucleotide biosynthesis genes, e.g. *SCO1483* (*pyrA*) or *SCO1485*. Independent transposon insertions at three distinct positions were found in *SCO1486* (*pyrC*). Also purine biosynthesis was frequently a target, and transposon insertions affecting proper sporulation were observed at two positions in *purL* (*SCO4079*), in *purM* (*SCO4087*), and in *purH* (*SCO4814*). Since chromosome replication is highly upregulated during the outgrowth of the aerial hyphae (Ruban-Ośmiałowska et al., 2006), it is conceivable that defects in nucleotide metabolism affect differentiation.

Interestingly, one of the transposon mutants affected in proper sporulation had an insertion in *SCO3110*, a gene previously identified in the BACTH screens (Table 1). The interaction with MreC and PkaI, the isolation from two independent BACTH libraries, as well as the impaired sporulation efficiency of the transposon insertion suggests a prominent role of SCO31110 in differentiation. The SCO3110/3111 transporter seems to be redundant in *S. coelicolor* A3(2), since SCO3089/3090 and SCO1031/1032 encode highly similar transporters. *SCO3110* was also identified by Hesketh et al., in a screen for *S. coelicolor* A3(2) genes becoming upregulated by antibiotics targeting cell wall synthesis (Hesketh et al., 2011). In this study, *SCO3110/3111* was 30-fold upregulated (together with SCO3089/3090). Whereas single mutants of these transporters showed a weak effect on bacitracin resistance, the double mutant strain exhibited markedly increased susceptibility to bacitracin, indicating a redundant function of these transporters in proper cell wall synthesis (Hesketh et al., 2011).

Three transposon insertions affecting sporulation were found in genes encoding putative exopolysaccharide phosphotransferases (SCO2592, SCO2594, and SCO6022), which show extensive sequence similarity to each other. These proteins probably function as hexose-1-phosphoryltransferases and might be involved in the biosynthesis of

Table 2
Transposon insertions affecting proper sporulation of *S. coelicolor* A3(2).

Tag*	Position of insertion	Predicted function
Nucleotide synthesis		
SCO1483	1587028	*pyrA*, carbamoylphosphate synthetase
SCO1485	1588592	membrane protein
SCO1486	1590157	dihydrorotase, pyrimidin synthesis
SCO1486	1589655	dihydrorotase, pyrimidin synthesis
SCO1486	1589379	dihydrorotase, pyrimidin synthesis
SCO4079	4472336	*purL*, phosphoribosyl formylglycinamidine synthase II
SCO4079	4473251	*purL*, phosphoribosyl formylglycinamidine synthase II
SCO4987	4481572	*purM,* phosphoribosylformylglycinamidine cyclo-ligase
SCO4091_	4485600	*bldC* region
SCO4814	5243085	*purH*, phosphoribosyl aminoimidazole carboxamide formyl transf.
Transcriptional regulation		
SCO1504	1608709	putative regulator
SCO1744	1864166	*abrA1*, two-component sensor histidine kinase
SCO2730	2976597	possible regulator
SCO2792	3047470	*adpA* regulator,γ-butyrolactone-responsive
SCO3361	3720344	*lrpA*, probable AsnC-family transcriptional regulator
SCO3579	3957624	WblA, WhiB family Regulator
SCO4190	4599321	*devA*, transcriptional regulator
SCO4197	4606699	possible MarR-family regulator
SCO4215	4623777	*xlnR*, GntR-regulator
SCO4895	5329300	possible ECF sigma factor
SCO4965	5400159	*greA,* transcription elongation factor
SCO5085	5528534	ActII-Orf4 Regulator
SCO5357	5826787	*rho*, transcriptional termination factor
SCO5511	6002908	phosphodiesterase, diGMP metabolizing
SCO5621	6121475	*whiG*, RNA polymerase sigma factor
SCO5704	6215605	*nusA* transcriptional termination/ antitermination factor
SCO5755	6293132	*clgR,* transcriptional regulator
SCO6268	6893643	possible histidine kinase
SCO6609_	7330209	*lrpA*, probable AsnC-family transcriptional regulator
SCO7297	8104527	possible two-component sensor histidine kinase
Antibiotic biosynthesis		
SCO3232	3578691	*cdaPS3*, CDA peptide synthetase III
SCO5088	5531744	actinorhodin polyketide beta-ketoacyl synthase beta subunit
SCO7682	8511758	non-ribosomal peptide synthase
Capsular polysaccharide biosynthesis		
SCO2592	2806241	capsular polysaccharide phosphotransferases, PhoP dependent
SCO2594	2809040	capsular polysaccharide phosphotransferases, PhoP dependent
SCO6022	6605756	exopolysaccharide phosphotransferase
Other function		
SCO0764	809009	(1- > 3)-beta-glucan endohydrolase
SCO0764	809610	(1- > 3)-beta-glucan endohydrolase
SCO0917	962398	luciferase family oxidoreductase
SCO1357	1435022	hypothetical protein
SCO1469	1569116	serine protease
SCO1663	1784136	probable cysteinyl-tRNA synthetase
SCO1751	1871449	sugar transporter
SCO1851	1984186	*cobO*, cob(I)alamin adenosyltransferase
SCO1857	1990631	probable bifunctional protein (CbiGH), cobalamin biosynthesis
SCO1867	2001360	possible ectoine hydroxylase
SCO1899	2034522	ABC sugar transporter (sorbitol)
SCO1965	2104421	possible export associated protein
SCO2153	2315587	possible secreted protein
SCO2512_	2709448	operon with *uppS* (undecaprenyl phosphate synthetase)
SCO2672	2910036	possible membrane protein
SCO2758	3005654	*nagA*, beta-N-acetylglucosaminidase
SCO3104	3400775	type II restriction endonuclease subunit
SCO3110	3408997	ABC-Transporter
SCO3285	3631169	large glycine/alanine rich protein
SCO3550	3925868	possible helicase
SCO3820	4199037	*pksC,* probable serine/threonine protein kinase

(*continued on next page*)

Table 2 (*continued*)

Tag*	Position of insertion	Predicted function
SCO4240	4645919	*msiK* sn-glycerol-3-phosphate transport ATP-binding protein
SCO4248	4655746	hypothetical protein, BldD controlled
SCO4253	4661476	phage tail protein, BldD dependent
SCO4293	4708983	*thrC*, threonine synthase
SCO4293	4708934	*thrC*, threonine synthase
SCO4498	4917165	probable proton transport protein
SCO4540_	4957556	multispecies protein
SCO4606	5029605	NADH dehydrogenase subunit NuoL2
SCO4700	5126942	hypothetical protein
SCO5354	5823283	*thrA*, homoserine dehydrogenase
SCO6383_	7049339	integral membrane protein
SCO6392	7059795	probable transposase
SCO6640	7376046	probable ATP-dependent helicase

* indicates Tn insertion upstream of the coding sequence.

exopolysaccharides. Such proteins are also called stealth proteins, since they help pathogenic bacteria to elude the host innate immune system. From six similar putative exopolysaccharide phosphotransferase genes of *S. coelicolor* A3(2) (*SCO2592, SCO2594, SCO6021, SCO6022, SCO6023, SCO6024*) three genes were inactivated by a transposon insertion (Table 2). Among these, the transposon insertion in *SCO6022* had the most severe phenotype resulting in very poor sporulation. The localization of *SCO2594* and *SCO2592* next to two TagF-like glycerophosphotransferase genes (*SCO2589, SCO2590*), the *tagTUV*-like *SCO2578* and the SSSC gene *SCO2584* supports a role of SCO2592 and SCO2594 in the synthesis of CWGs. Also, the predicted *SCO6021-6025* operon is preceded by the *tagTUV*-like *SCO6020*, suggesting that the polysaccharide synthesized by these enzymes is linked to the muramic acid of the PG by the SCO6020 transferase.

5. Cell Wall Glycopolymers (CWGs) and the composition of the spore envelope of *S. coelicolor* A3(2)

Van der Aart and coworkers compared the PG compositions of spores and vegetative mycelia of *S. coelicolor* A3(2) by LC-MS analyses of muropeptides (van der Aart et al., 2018). Spore walls contained an increased amount (44%) of tetrapeptides, compared to 23%–25% tetrapeptides in PG of vegetative mycelium (Table3). The increase in tetrapeptides correlates with the formation of 3-3 cross-links, which require tetrapeptides, rather than pentapeptides, as a substrate. In agreement, 35% of the dimers from spore PG were 3-3 cross-linked. Conversely, only 5% of the spore muropeptide monomers were pentapeptides, while vegetative PG contained 10%–22% pentapeptides. Moreover, a tripeptide which lacks GlcNAc and contains a deacetylated MurNAc (MurN-Tri) made up 3.5% of the muropeptide monomers of spore PG (van der Aart et al., 2018). *N*-deacetylation of PG strands is widespread among bacteria and is commonly linked to lysozyme resistance (Meyrand et al., 2007). Taken together, these structural modifications of the spore PG probably contribute to the structural stability of *S. coelicolor* A3(2) spores.

To compare their CWG composition, cell envelopes from *S. coelicolor* A3(2) vegetative mycelium and spores were isolated according to Schäberle et al. (2011). Subsequently, the attached CWGs were separated from the PG by acidic hydrolysis. These analyses revealed that spore walls contained reduced amounts of CWGs: whereas cell walls of vegetative mycelium consisted of 64% PG and 36% CWGs, spore walls consisted of 78% PG and only 22% CWGs (Sigle et al., 2016b). This demonstrates that *S. coelicolor* A3(2) remodels its cell wall during differentiation, either by increasing the amount of PG or by removing CWGs (or both).

CWGs are synthesized on a sugar linker unit, which is attached to the muramic acid of PG via a phosphoester bond. Shashkov et al. characterized the CWGs of vegetatively grown *S. coelicolor* A3(2) (Shashkov et al., 2012). In their analyses, Shashkov and coworkers did not observe classical glycerol- or ribitolphosphate containing wall teichoic acids, but identified a phosphate free teichulosonic acid as a major CWG. The teichulosonic acid consists of up to seven repeating units of galactose (Gal) linked to the sialinic acid sugar 2-keto-3-deoxy-D-glycero-D-galacto-nononic acid (Kdn), often substituted with N-actylglucosamine (GlcNAc) or a methyl group. They also found a diglycosylphosphate polymer (PDP) of Gal and GlcNAc-phosphate as a minor component (Shashkov et al., 2012). Genes (*SCO4879-SCO4882*) directing the synthesis of the Kdn sugar have been identified in the genomic sequence of *S. coelicolor* A3(2) and inactivated. The respective mutant did no longer produce teichulosonic acid, but accumulated the minor CWG component PDP (Ostash et al., 2014).

To distinguish the two CWGs, teichulosonic acid and PDP, photometric assays to determine specific CWG components were developed. PDP was quantified by the determination of the phosphate content of the CWG fraction, the amount of teichulosonic acid was calculated by determining the amount of Kdn. In addition, the amount of hexosamines, present in PDP, teichulosonic acid, and probably in the not yet known linker unit was quantified (Sigle et al., 2016b). Whereas the Kdn content of spore walls (80 nmol/mg) was only slightly lower than that of vegetative mycelium (95 nmol/mg), the phosphate content of spore wall glycopolymers (88 nmol/mg) showed a reduction of 49% compared to that of vegetative cell walls (172 nmol/mg). Therefore it

Table 3
Composition of cell envelopes of vegetative mycelium and spores.

Component	Vegetative mycelium	Spores	Reference
PG-crosslinking			
Tetrapeptides in PG	23-25%	44%	van der Aart et al., 2018
Pentapeptides in PG	10-22%	5%	
Cell wall glycopolymer composition			
CWG content	36%	22%	Sigle et al., 2016b
Kdn content	95 nmol/mg	80 nmol/mg	
Phosphate content	172 nmol/mg	88 nmol/mg	
PAGE of partially hydrolyzed CWGs			
Band pattern	Widely spaced(Fig. 3., left lane)	Narrow spaced(Fig.3, right lane)	Steblau et al., unpublished
HPLC-MS analysis of hydrolyzed CWGs*			
GalKdn-R (teichulosonic acid)R= H (431.14 $[M+H]^+$)R = CH_3 (445.16 $[M+H]^+$)R = GlcNAc (634.22 $[M+H]^+$)	+	+	Steblau et al., unpublished
GalGlcNAcP (PDP) 464.12 $[M+H]^+$	+	+/-	

* Hydrolyzed CWG fragments were separated by reversed-phase HPLC on a Gemini C18 column (Phenomenex) with a 0–40% acetonitrile gradient. Masses were detected by ESI-MS, micro-TOF (Bruker Daltonics) in the positive mode (range 200–2000 m/z), as described in Borisova et al. (2016). (+) indicates prominent peaks, (+/-) indicates peak detected only in minute amounts.

was suggested that spore walls contain significantly lower amounts of PDP (Sigle et al., 2016b).

HPLC-MS analysis (Gemini C18 column, Phenomenex) of hydrolyzed CWGs (50 mM HCl, 5–15 min, 90 °C) detected peaks corresponding to Kdn monomers substituted with either H (431.14 $[M+H]^+$), CH_3 (445.16 $[M+H]^+$), or GlcNAc (634.22 $[M+H]^+$) in CWG samples of vegetative mycelium and of spores (Table 3, Steblau and Walter, unpublished). Thus, teichulosonic acid is not only present in the cell walls of vegetative mycelium, but is also a component of spore envelopes. Moreover, a prominent peak of the mass of the PDP monomer (464.12 $[M+H]^+$) was detected in the CWGs of vegetative mycelium. Also, a second peak corresponding to the PDP dimer (909.22 $[M+H]^+$) was present in the same intensity as the monomer peak at short hydrolysis conditions (5 min). During prolonged hydrolysis (> 10 min) the PDP dimer peak disappeared and the PDP monomer peak increased in intensity. In contrast, only a very small PDP monomer peak was found in hydrolyzed CWGs of spore envelopes (Steblau and Walter, unpublished). These findings confirmed the analyses of Shaskov et al. and revealed the existence of both polymers, teichulosonic acid and PDP in vegetative mycelium. In spores only teichulosonic acid was reliably detected. The small PDP peak in the spore wall hydrolysate could also result from a possible contamination of spore walls with remains of aerial hyphae.

Chain length of the CWGs of vegetative mycelium and spores were analyzed and compared by high resolution PAGE analyses. CWGs were partially hydrolyzed by mild acidic conditions (Sigle et al., 2016b), expected to selectively hydrolyze phosphoester bonds, and the resulting CWG fragments of increasing length were separated on a 40 cm acrylamide (20%) gel. A combined alcian blue/silver staining visualized ladder-like fragment patterns (Fig. 3). The non-uniform distances within the fragment patterns in the lower and upper parts of the gel indicates that the CWGs of vegetative mycelium are a mixture of two different polymers, hindering an exact calculation of the CWG chain length. Comparing the fragment pattern of mycelial CWGs with that of spore CWGs in the lower part of the gel showed clear differences (N. Steblau, unpublished results). Whereas, the spore CWG fragments were narrow spaced, the distance of the mycelial CWG bands was much larger (Fig. 3.). This implies that the mycelial CWG and the spore CWG contain different subunits and that the CWG from vegetative mycelium is composed of larger subunits compared to the spore CWG. The differences in the envelope compositions of vegetative mycelium and spore envelopes are summarized in Table 3.

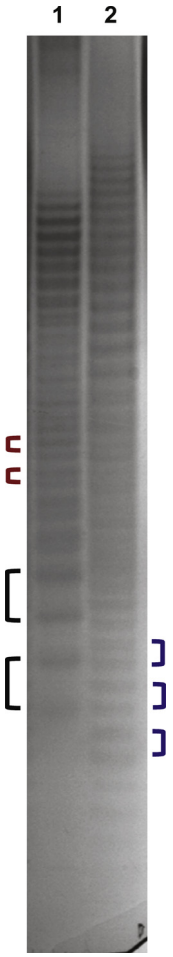

Fig. 3. PAGE analysis of *S. coelicolor* cell wall glycopolymers (CWGs). CWGs from vegetative mycelium (1) and spore envelopes (2) were hydrolyzed under mild acidic conditions (15 min 50 mM HCl). The resulting CWG fragments were separated on a 40 cm polyacrylamide gel (20%) at 18 mA for 7 h and stained with alcian blue/silver. The shown images are representative results of biological replicate experiments. Black and red brackets mark distinct fragment patterns in the CWGs of vegetative mycelium, indicating a mixture of two polymers. Blue brackets mark the distance of the spore CWG fragments.

6. Distinct role of PdtA (SCO2578) in the life cycle of *S. coelicolor* A3(2)

The LytR-CpsA-Psr (LCP) protein SCO2578 (PdtA), which was identified as a SSSC protein and which is predicted to anchor exopolysaccharides or CWGs to the muramic acid of PG was deleted (Sigle et al., 2016a). Despite the presence of 10 additional LCP-homologues in *S. coelicolor* A3(2), the resulting *ΔpdtA* mutant showed severe defects. First, integrity of the spore envelope was affected and 34% nonviable spores were produced. This defect coincided with a reduced phosphate content in the spore envelope, leading to the conclusion that the amount of PDP (or an unknown CWG) was reduced (Sigle et al., 2016a). Second, apical tip extension and normal branching of vegetative mycelium was impaired and staggered extensions with a bulbous morphology were formed. The defect was more dramatic under osmotic stress, when the *ΔpdtA* mutant was grown on LB agar supplemented with 6% NaCl. Instead of normal branches occurring in a distance of more than 20–30 µm to the tip, all hyphal tips of the *ΔpdtA* mutant showed hyperbranching directly at the tips without further extension growth, resulting in a bulky and dented mycelium (Sigle et al., 2016a). Localization of the sites of peptidoglycan synthesis by BODIPY FL Vancomycin (Van-fl) staining, revealed an aberrant PG-incorporation pattern. The mislocalization of PG-synthesis and the morphology of the aberrant hyphae suggested a defect in the tip localized PG-synthesis apparatus. As a consequence of the blocked tip extension, new tips are established close by, which also fail to elongate into normal hyphae. Therefore, PdtA itself or the CWG attached to the PG by the glycopolymer transferase PdtA is not only required for proper sporulation, but also has a crucial function in apical tip extension of vegetative hyphae under stress conditions (Fig. 4).

7. Control of differentiation by protein-phosphorylation

A crucial step in *Streptomyces* differentiation is the simultaneous formation of dozens of cross walls in the aerial hyphae. During sporulation septation the membrane- and PG-synthesizing machineries, including the SSSC, have to be provided in sufficient quantities and positioned properly. Moreover, the activities of the complexes have to be controlled to prevent aberrant sporulation by sporadic formation of single cross walls in a non-coordinated manner.

Controlling activity of proteins involved in cell division and cell wall synthesis by phosphorylation is a well-documented regulatory mechanism in many bacteria (Molle and Kremer, 2010; Hempel et al., 2012; Jarick et al., 2018; Sharma et al., 2016). However, phosphorylation of one of the Mre proteins has not been reported yet in any

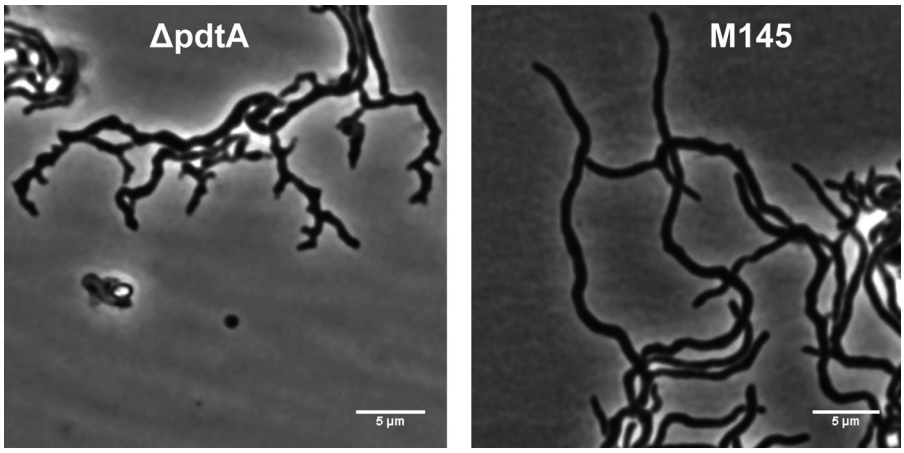

Fig. 4. Aberrant branching of the *ΔpdtA* mutant under osmotic stress. *ΔpdtA* (left) and M145 (right) were grown for 72 h on LB-agar, supplemented with 6% NaCl. In contrast to the wild type M145, the *ΔpdtA* mutant shows hyperbranching and blocked elongation of the hyphae. The shown images are representative results of biological replicate experiments.

bacterium. The discovery that the eSTPK PkaI, which is encoded in a cluster of five consecutive eSTPK genes (*SCO4775 (pkaH), SCO4776, SCO4777 (pkaD), SCO4778 (pkaI), and SCO4779 (pkaJ)*, had a central position in the SSSC interaction network (Kleinschnitz et al., 2011a), provided first evidence that the activity of the SSSC might be regulated by protein phosphorylation. Next it was shown that depletion of phosphorylation activity by inactivating *pkaI* or by deleting all five eSTPK genes affected sporulation. But also expressing a second copy of any one of the five eSTPK genes under control of its native promoter caused an even more severe phenotype. Aberrant spore chains were formed, containing irregular sized spore, dead spores, or spores without DNA. Moreover, the germinating spores were sensitive to osmotic stress and cell wall damage by lysozyme or vancomycin (Ladwig et al., 2015). Thus it was concluded that the balanced phosphorylation activity is crucial for proper sporulation.

To study whether PkaI or one of the other eSTPKs phosphorylate SSSC proteins, all five eSTPK genes were cloned into pCDF-Duet, fused to an N-terminal his-tag encoding sequence, and coexpressed with *mreC* fused to a C-terminal S-tag encoding sequence (Vollmer, unpublished results). Following induction of gene expression, the phosphorylation status of eSTPK-His and MreC-Stag was studied by phosphostaining with ProQ diamond. Whereas MreC_S-tag was non-phosphorylated, when purified in the absence of one of the eSTPKs, it was phosphorylated, when it was coexpressed with either *pkaI* or *pkaH* (Ladwig et al., 2015, Vollmer, unpublished results).

The phosphosites of PkaI and MreC were identified using purified proteins, subjected to proteolytic digestion and analyses of the resulting peptide masses by LC-MS/MS (Ladwig et al., 2015). Two phosphorylated peptides, $PkaI_{111\text{-}124}$ (VL**pT**RGPVDAVEAAR) and $PkaI_{164\text{-}177}$ (FGVAQVAGA**p[TT]**LTE) were identified for PkaI. $PkaI_{164\text{-}177}$ corresponds to the so-called activation loop of eSTPKs, involved in determining substrate specificity (Pereira et al., 2011).

For MreC, a single peptide ($MreC_{219\text{-}251}$, LVTFGSQADKPFVPGVPVGp[**TIT**]RVDPNGGDLTR), derived from the Pfam_MreC domain ($MreC_{121\text{-}273}$), was detected 100-fold more abundant in the phosphorylated form compared to the non-phosphorylated one. The fragmentation spectrum did not allow an unambiguous assignment of the phosphorylation to one of the two threonine (**T_{238}, T_{240}**) residues. T_{238}/T_{240} of MreC was only phosphorylated with low efficiency by PkaH, whereas T_{250} was identified as its major phosphosite within MreC (Vollmer, unpublished results).

When *pbp2* was coexpressed with *pkaI*, PBP2 was only detected in the presence of PkaI, indicating that expression of *pbp2* was detrimental to the cell and only tolerated, when *pkaI* was coexpressed, resulting in phosphorylated PBP2. Four phosphorylated peptides were detected by LC-MS/MS: $PBP2_{72\text{-}81}$ (GVALADNEp**T**R), $PBP2_{82\text{-}93}$ (LVV**p[SASRT]**DLLK), $PBP2_{210\text{-}220}$ (SDQVGR**pS**GLER), and $PBP2_{550\text{-}560}$ (AVVSPDGK**pT**VR). Presence of three phosphosites in the N-terminal dimerization domain ($PBP2_{60\text{-}250}$) indicates that PBP2 phosphorylation affects its dimerization (Ladwig et al., 2015).

The effect of eSTPK expression/deletion on proper sporulation, the protein-protein interaction pattern of PkaI, as well as the specific phosphorylation of MreC by PkaI and PkaH suggest that all eSTPKs of the cluster are involved in the regulatory network controlling SSSC activity (Fig.5).

Based on these findings a model was developed, in which coordinated sporulation septation and synthesis of the spore envelope is triggered by the phosphorylation status of SSSC proteins (Fig. 6). In this model, some of the SSSC proteins are phosphorylated in the early phases of aerial hyphae development by the different eSTPKs to keep them inactive and to prevent the premature assembly of SSSC complexes. After the outgrowth of the aerial hyphae is completed and sufficient amounts of SSSC proteins have been synthesized and positioned, the SSSC proteins become activated by dephosphorylation (involving phosphatases). As a consequence they can form functional SSSC complexes for the coordinated synthesis of sporulation septa and spore envelopes.

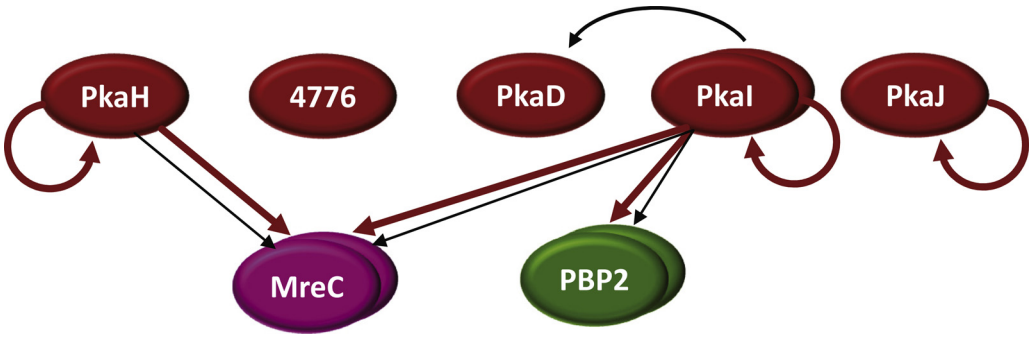

Fig. 5. Phosphorylation of the SSSC proteins MreC and PBP2 by multiple eSTPKS. eSTPKs, which were shown to affect proper sporulation are drawn as red ellipses. Red arrows indicate phosphorylation detected by ProQ diamond staining or LC-MS/MS, while a black arrow marks protein-protein interaction shown by co-purification or BACTH analyses (Ladwig et al., 2015, Vollmer et al., unpublished results). Self-interactions are indicated by double ellipses.

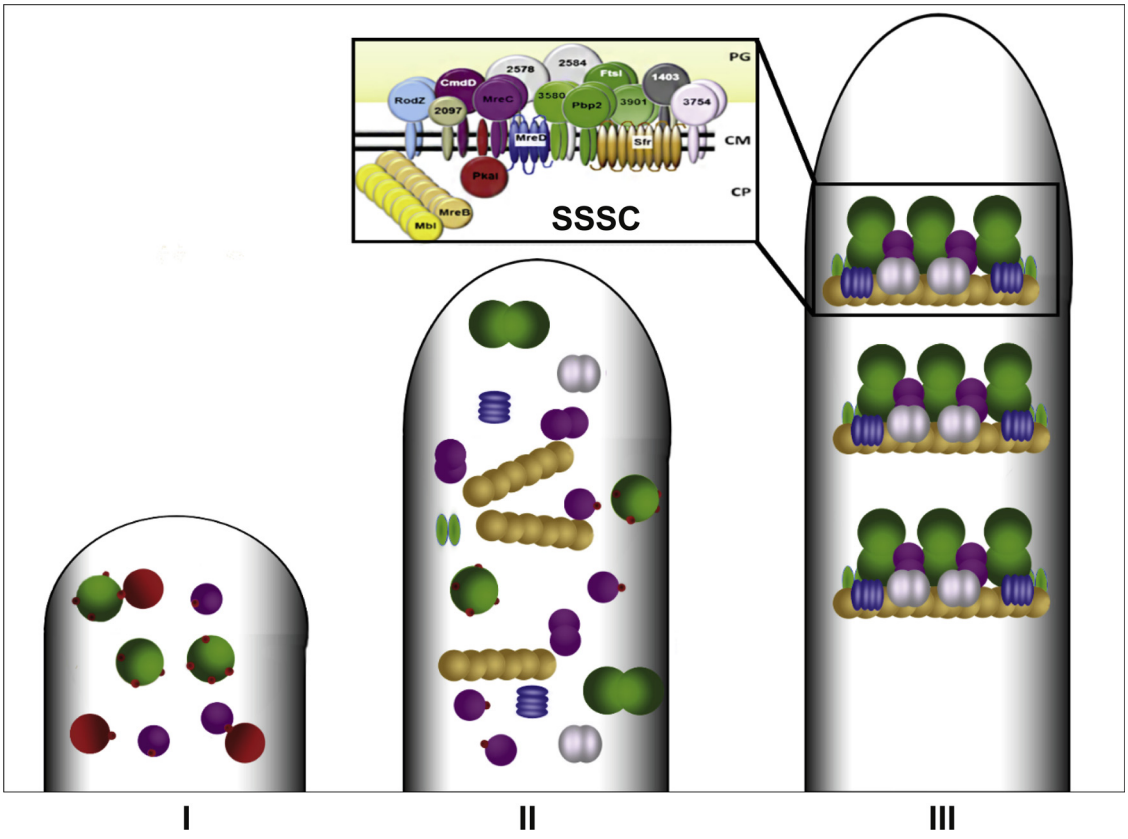

Fig. 6. Coordination of synchronized sporulation septation and synthesis of the thickened spore envelope by the phosphorylation of SSSC proteins. In this model, eSTPKs phosphorylate untimely expressed SSSC proteins (I-II) to prevent their premature assembly, which would result in non-coordinated septum synthesis. After completion of aerial hyphae growth (III), the phosphorylated SSSC proteins become dephosphorylated by phosphatases and functional SSSC complexes can assemble to build sporulation septa in a synchronized manner.

Acknowledgements

This work was supported by the Deutsche Forschungsgemeinschaft: SFB766

References

Ausmees, N., Wahlstedt, H., Bagchi, S., Elliot, M.A., Buttner, M.J., Flardh, K., 2007. SmeA, a small membrane protein with multiple functions in *Streptomyces* sporulation including targeting of a SpoIIIE/FtsK-like protein to cell division septa. Mol. Microbiol. 65, 1458–1473.

Borisova, M., Gaupp, R., Duckworth, A., Schneider, A., Dalügge, D., Mühleck, M., Deubel, D., Unsleber, S., Yu, W., Muth, G., Bischoff, M., Götz, F., Mayer, C., 2016. Peptidoglycan recycling in Gram-positive bacteria is crucial for survival in stationary phase. MBio 7, e00923–16.

Bush, M.J., Tschowri, N., Schlimpert, S., Flärdh, K., Buttner, M.J., 2015. c-di-GMP signalling and the regulation of developmental transitions in streptomycetes. Nat. Rev. Microbiol. 13, 749–760.

Burger, A., Sichler, K., Kelemen, G., Buttner, M., Wohlleben, W., 2000. Identification and characterization of the *mre* gene region of *Streptomyces coelicolor* A3(2). Mol. Gen. Genet. 263, 1053–1060.

Claessen, D., Stokroos, I., Deelstra, H.J., Penninga, N.A., Bormann, C., Salas, J.A., Dijkhuizen, L., Wosten, H.A., 2004. The formation of the rodlet layer of streptomycetes is the result of the interplay between rodlins and chaplins. Mol. Microbiol. 53, 433–443.

Colson, S., van Wezel, G.P., Craig, M., Noens, E.E., Nothaft, H., Mommaas, A.M., Titgemeyer, F., Joris, B., Rigali, S., 2008. The chitobiose-binding protein, DasA, acts as a link between chitin utilization and morphogenesis in *Streptomyces coelicolor*. Microbiology 154, 373–382.

Crow, A., Greene, N.P., Kaplan, E., Koronakis, V., 2017. Structure and mechanotransmission mechanism of the MacB ABC transporter superfamily. Proc. Natl. Acad. Sci. U.S.A. 114, 12572–12577.

Del Sol, R., Pitman, A., Herron, P., Dyson, P., 2003. The product of a developmental gene, *crgA*, that coordinates reproductive growth in *Streptomyces* belongs to a novel family of small actinomycete-specific proteins. J. Bacteriol. 185, 6678–6685.

Dominguez-Escobar, J., Chastanet, A., Crevenna, A.H., Fromion, V., Wedlich-Soldner, R., Carballido-Lopez, R., 2011. Processive movement of MreB-associated cell wall biosynthetic complexes in bacteria. Science 333, 225–228.

Divakaruni, A.V., Baida, C., White, C.L., Gober, J.W., 2007. The cell shape proteins MreB and MreC control cell morphogenesis by positioning cell wall synthetic complexes. Mol. Microbiol. 66, 174–188.

Du, S., Pichoff, S., Lutkenhaus, J., 2016. FtsEX acts on FtsA to regulate divisome assembly and activity. Proc. Natl. Acad. Sci. U.S.A. 113, 5052–5061.

Eccleston, M., Ali, R.A., Seyler, R., Westpheling, J., Nodwell, J., 2002. Structural and genetic analysis of the BldB protein of *Streptomyces coelicolor*. J. Bacteriol. 184, 4270–4276.

Elliot, M.A., Karoonuthaisiri, N., Huang, J., Bibb, M.J., Cohen, S.N., Kao, C.M., Buttner, M.J., 2003. The chaplins: a family of hydrophobic cell-surface proteins involved in aerial mycelium formation in *Streptomyces coelicolor*. Genes Develop 17, 1727–1740.

Flardh, K., 2003. Growth polarity and cell division in *Streptomyces*. Curr. Op. Microbiol. 6, 564–571.

Flardh, K., Buttner, M.J., 2009. *Streptomyces* morphogenetics: dissecting differentiation in a filamentous bacterium. Nat. Rev. Microbiol. 7, 36–49.

Flardh, K., Richards, D.M., Hempel, A.M., Howard, M., Buttner, M.J., 2012. Regulation of apical growth and hyphal branching in Streptomyces. Curr. Op. Microbiol. 15, 737–743.

Formstone, A., Carballido-Lopez, R., Noirot, P., Errington, J., Scheffers, D.J., 2008. Localization and interactions of teichoic acid synthetic enzymes in *Bacillus subtilis*. J. Bacteriol. 190, 1812–1821.

Garner, E.C., Bernard, R., Wang, W., Zhuang, X., Rudner, D.Z., Mitchison, T., 2011. Coupled, circumferential motions of the cell wall synthesis machinery and MreB filaments in B. Subtilis. Science. 333, 222–225.

Heichlinger, A., Ammelburg, M., Kleinschnitz, E.M., Latus, A., Maldener, I., Flardh, K., Wohlleben, W., Muth, G., 2011. The MreB-like protein Mbl of *Streptomyces coelicolor* A3(2) depends on MreB for proper localization and contributes to spore wall synthesis. J. Bacteriol. 193, 1533–1542.

Hempel, A.M., Cantlay, S., Molle, V., Wang, S.B., Naldrett, M.J., Parker, J.L., Richards, D.M., Jung, Y.G., Buttner, M.J., Flardh, K., 2012. The Ser/Thr protein kinase AfsK regulates polar growth and hyphal branching in the filamentous bacteria *Streptomyces*. Proc. Natl. Acad. Sci. U.S.A. 109, 2371–2379.

Hesketh, A., Hill, C., Mokhtar, J., Novotna, G., Tran, N., Bibb, M., Hong, H.J., 2011. Genome-wide dynamics of a bacterial response to antibiotics that target the cell envelope. BMC Genomics 12, 226.

Jakimowicz, D., Gust, B., Zakrzewska-Czerwinska, J., Chater, K.F., 2005. Developmental-stage-specific assembly of ParB complexes in *Streptomyces coelicolor* hyphae. J. Bacteriol. 187, 3572–3580.

Jarick, M., Bertsche, U., Stahl, M., Schultz, D., Methling, K., Lalk, M., Stigloher, C., Steger,

M., Schlosser, A., Ohlsen, K., 2018. The serine/threonine kinase Stk and the phosphatase Stp regulate cell wall synthesis in *Staphylococcus aureus*. Sci. Rep. 8, 13693. https://doi.org/10.1038/s41598-018-32109-7.

Jyothikumar, V., Tilley, E.J., Wali, R., Herron, P.R., 2008. Time-lapse microscopy of *Streptomyces coelicolor* growth and sporulation. Appl. Environ. Microbiol. 74, 6774–6781.

Karimova, G., Pidoux, J., Ullmann, A., Ladant, D., 1998. A bacterial two-hybrid system based on a reconstituted signal transduction pathway. Proc. Natl. Acad. Sci. U.S.A. 95, 5752–5756.

Kelemen, G.H., Buttner, M.J., 1998. Initiation of aerial mycelium formation in *Streptomyces*. Curr. Op. Microbiol. 1, 656–662.

Kleinschnitz, E.M., Heichlinger, A., Schirner, K., Winkler, J., Latus, A., Maldener, I., Wohlleben, W., Muth, G., 2011a. Proteins encoded by the *mre* gene cluster in *Streptomyces coelicolor* A3(2) cooperate in spore wall synthesis. Mol. Microbiol. 79, 1367–1379.

Kleinschnitz, E.M., Latus, A., Sigle, S., Maldener, I., Wohlleben, W., Muth, G., 2011b. Genetic analysis of SCO2997, encoding a TagF homologue, indicates a role for wall teichoic acids in sporulation of *Streptomyces coelicolor* A3(2). J. Bacteriol. 193, 6080–6085.

Kruse, T., Bork-Jensen, J., Gerdes, K., 2005. The morphogenetic MreBCD proteins of *Escherichia coli* form an essential membrane-bound complex. Mol. Microbiol. 55, 78–89.

Ladwig, N., Franz-Wachtel, M., Hezel, F., Soufi, B., Macek, B., Wohlleben, W., Muth, G., 2015. Control of morphological differentiation of *Streptomyces coelicolor* A3(2) by phosphorylation of MreC and PBP2. PLoS One 10, e0125425.

Ma, H., Kendall, K., 1994. Cloning and analysis of a gene cluster from *Streptomyces coelicolor* that causes accelerated aerial mycelium formation in *Streptomyces lividans*. J. Bacteriol. 176, 3800–3811.

Meeske, A.J., Riley, E.P., Robinsm, W.P., Uehara, T., Mekalanosm, J.J., Kahnem, D., Walker, S., Kruse, A.C., Bernhardt, T.G., Rudner, D.Z., 2016. SEDS proteins are a widespread family of bacterial cell wall polymerases. Nature. 537, 634–638.

Meyrand, M., Boughammoura, A., Courtin, P., Mezange, C., Guillot, A., Chapot-Chartier, M.P., 2007. Peptidoglycan N-acetylglucosamine deacetylation decreases autolysis in Lactococcus lactis. Microbiology 153, 3275–3285.

Mazza, P., Noens, E.E., Schirner, K., Grantcharova, N., Mommaas, A.M., Koerten, H.K., Muth, G., Flardh, K., van Wezel, G.P., Wohlleben, W., 2006. MreB of *Streptomyces coelicolor* is not essential for vegetative growth but is required for the integrity of aerial hyphae and spores. Mol. Microbiol. 60, 838–852.

Molle, V., Kremer, L., 2010. Division and cell envelope regulation by Ser/Thr phosphorylation: *mycobacterium* shows the way. Mol. Microbiol. 75, 1064–1077.

Morgenstein, R.M., Bratton, B.P., Nguyen, J.P., Ouzounov, N., Shaevitz, J.W., Gitai, Z., 2015. RodZ links MreB to cell wall synthesis to mediate MreB rotation and robust morphogenesis. Proc Natl Acad Sci U S A. 112, 12510–12515.

Nothaft, H., Rigali, S., Boomsma, B., Swiatek, M., McDowall, K.J., van Wezel, G.P., Titgemeyer, F., 2010. The permease gene nagE2 is the key to N-acetylglucosamine sensing and utilization in *Streptomyces coelicolor* and is subject to multi-level control. Mol. Microbiol. 75, 1133–1144.

Ostash, B., Shashkov, A., Streshinskaya, G., Tul'skaya, E., Baryshnikova, L., Dmitrenok, A., Dacyuk, Y., Fedorenko, V., 2014. Identification of *Streptomyces coelicolor* M145 genomic region involved in biosynthesis of teichulosonic acid-cell wall glycopolymer. Folia Microbiol. (Praha) 59, 355–360.

Pereira, S.F., Goss, L., Dworkin, J., 2011. Eukaryote-like serine/threonine kinases and phosphatases in bacteria. Microbiol. Mol. Biol. Rev. 75, 192–212.

Poralla, K., Muth, G., Hartner, T., 2000. Hopanoids are formed during transition from substrate to aerial hyphae in *Streptomyces coelicolor* A3(2). FEMS Microbiol. Lett. 189, 93–95.

Reznikoff, W.S., 2008. Transposon Tn*5*. Annu. Rev. Genet. 42, 269–286.

Richards, D.M., Hempel, A.M., Flardh, K., Buttner, M.J., Howard, M., 2012. Mechanistic basis of branch-site selection in filamentous bacteria. PLoS Comput. Biol. 8, e1002423.

Ruban-Ośmiałowska, B., Jakimowicz, D., Smulczyk-Krawczyszyn, A., Chater, K.F., Zakrzewska-Czerwińska, J., 2006. Replisome localization in vegetative and aerial hyphae of *Streptomyces coelicolor*. J. Bacteriol. 188, 7311–7316.

Salerno, P., Persson, J., Bucca, G., Laing, E., Ausmees, N., Smith, C.P., Flardh, K., 2013. Identification of new developmentally regulated genes involved in *Streptomyces coelicolor* sporulation. BMC Microbiol. 13, 281.

Schäberle, T.F., Vollmer, W., Frasch, H.J., Huttel, S., Kulik, A., Rottgen, M., von Thaler, A.K., Wohlleben, W., Stegmann, E., 2011. Self-resistance and cell wall composition in the glycopeptide producer *Amycolatopsis balhimycina*. Antimicrob. Agents Chemother. 55, 4283–4289.

Schlimpert, S., Flardh, K., Buttner, J., 2016. Fluorescence time-lapse imaging of the complete *S. Venezuelae* life cycle using a microfluidic device. J. Vis. Exp. 108, E53863.

Schlimpert, S., Wasserstrom, S., Chandra, G., Bibb, M.J., Findlay, K.C., Flardh, K., Buttner, M.J., 2017. Two dynamin-like proteins stabilize FtsZ rings during *Streptomyces* sporulation. Proc. Natl. Acad. Sci. U.S.A. 114, 6176–6183.

Seo, J.W., Ohnishi, Y., Hirata, A., Horinouchi, S., 2002. ATP-binding cassette transport system involved in regulation of morphological differentiation in response to glucose in *Streptomyces griseus*. J. Bacteriol. 184, 91–103.

Sharma, A.K., Arora, D., Singh, L.K., Gangwal, A., Sajid, A., Molle, V., Singh, Y., Nandicoori, V.K., 2016. Serine/Threonine protein phosphatase PstP of *Mycobacterium tuberculosis* is necessary for accurate cell division and survival of pathogen. J. Biol. Chem. 291, 24215–24230.

Shashkov, A.S., Ostash, B.E., Fedorenko, V.A., Streshinskaya, G.M., Tul'skaya, E.M., Senchenkova, S.N., Baryshnikova, L.M., Evtushenko, L.I., 2012. Novel teichulosonic acid from cell wall of *Streptomyces coelicolor* M145. Carbohydr. Res. 359, 70–75.

Shu, D., Chen, L., Wang, W., Yu, Z., Ren, C., Zhang, W., Yang, S., Lu, Y., Jiang, W., 2009. afsQ1-Q2-sigQ is a pleiotropic but conditionally required signal transduction system for both secondary metabolism and morphological development in *Streptomyces coelicolor*. Appl. Microbiol. Biotechnol. 81, 1149–1160.

Sigle, S., Steblau, N., Wohlleben, W., Muth, G., 2016a. Polydiglycosylphosphate transferase PdtA (SCO2578) of *Streptomyces coelicolor* A3(2) is crucial for proper sporulation and apical tip extension under stress conditions. Appl. Environ. Microbiol. 82, 5661–5672.

Sigle, S., Steblau, N., Wohlleben, W., Muth, G., 2016b. A toolbox to measure changes in the cell wall glycopolymer composition during differentiation of *Streptomyces coelicolor* A3(2). J. Microbiol. Methods 128, 52–57.

Taguchi, A., Welsh, M.A., Marmont, L.S., Lee, W., Sjodt, M., Kruse, A.C., Kahne, D., Bernhardt, T.G., Walker, S., 2019. FtsW is a peptidoglycan polymerase that is functional only in complex with its cognate penicillin-binding protein. Nat. Microbiol. 4, 587–594.

van der Aart, L.T., Spijksma, G.K., Harms, A., Vollmer, W., Hankemeier, T., van Wezel, G.P., 2018. High-resolution analysis of the peptidoglycan composition in *Streptomyces coelicolor*. J. Bacteriol. 200, e00290–18. https://doi.org/10.1128/JB.00290-18.

Wang, L., Yu, Y., He, X., Zhou, X., Deng, Z., Chater, K.F., Tao, M., 2007. Role of an FtsK-like protein in genetic stability in *Streptomyces coelicolor* A3(2). J. Bacteriol. 189, 2310–2318.

Willemse, J., Borst, J.W., de Waal, E., Bisseling, T., van Wezel, G.P., 2011. Positive control of cell division: FtsZ is recruited by SsgB during sporulation of *Streptomyces*. Genes Dev. 25, 89–99.

Xu, Z., Wang, Y., Chater, K.F., Ou, H.Y., Xu, H.H., Deng, Z., Tao, M., 2017. Large-scale transposition mutagenesis of *Streptomyces coelicolor* identifies hundreds of genes influencing antibiotic biosynthesis. Appl. Environ. Microbiol. 83, e02889–16.